




Distinctive onset of electron correlation in molecular tautomersKalyani Chordiya ^{1,2}, Victor Despré ³, Mousumi U. Kahaly^{1,2,*} and Alexander I. Kuleff ^{1,3,†}¹*ELI-ALPS, ELI-HU Non-Profit Ltd., Wolfgang Sandner utca 3, Szeged, H-6728, Hungary*²*Institute of Physics, University of Szeged, Dóm tér 9, H-6720 Szeged, Hungary*³*Theoretische Chemie, Universität Heidelberg, Im Neuenheimer Feld 229, D-69120 Heidelberg, Germany*

(Received 7 February 2022; accepted 18 May 2022; published 10 June 2022)

We investigate the attosecond response of the electronic cloud of a molecular system to an outer-valence ionization. The time needed for the remaining electrons to respond to a sudden perturbation in the electronic structure of the molecule is a measure of the degree of electron correlation. Using the *ab initio* multielectron wave-packet propagation method, we analyze the ultrafast many-body dynamics following the removal of different outer-valence electrons of two tautomers of the uracil molecule and show that this response time can be sensitive to the molecular structure and the symmetry of the ionized molecular orbital.

DOI: [10.1103/PhysRevA.105.062808](https://doi.org/10.1103/PhysRevA.105.062808)**I. INTRODUCTION**

Governed by the long-range Coulomb interaction, the motion of the electrons in atoms and molecules is correlated. As a result, perturbations to a single electron are felt by the whole electronic cloud even in extended systems. The response of the system to the changes introduced by the perturbation often involves rearrangements in its electronic structure. The electron correlation is thus the driving force of a plethora of processes taking place in many-electron systems [1], with autoionization [2], population of satellite states upon ionization [3], energy transfer [4,5], and charge migration [6,7] being just a few examples of such electron-correlation effects. That is why, over the years, electron correlation and the processes driven by it have been a subject of intensive research, both by theory and experiment. So far they have been mainly investigated in the energy domain, where direct access to the full quantum information (amplitudes and phases) is often difficult. However, with the advent of attosecond pulse generation techniques [8] and the possibility to perform pump-probe experiments with extreme temporal resolution [9], the scientific community obtained a powerful tool to analyze and study electron-correlation processes directly in time.

One of the important questions in this respect is how fast does the electronic cloud respond to the process-triggering perturbation? Or, in other words, what is the timescale of the electron correlation and how much it is system specific? In their seminal paper [10], Breidbach and Cederbaum studied this question by investigating the response of a many-electron system to a sudden removal of one of its electrons. They showed that the time needed for the electronic cloud to respond to a sudden ionization is about 50 attoseconds ($1 \text{ as} = 10^{-18} \text{ s}$) and that this time is nearly independent of the system. Due to the characteristic evolution of the density of the

created hole charge, this universal time was interpreted as the timescale of the filling of the exchange-correlation hole of the removed electron. The exchange-correlation hole represents the region of space around each electron where the probability to find another electron is close to zero due to the quantum exchange and correlation effects [11]. Although the time for filling of the exchange-correlation hole of an initially created vacancy might be universal, it is not the shortest response time of the electronic cloud to a sudden ionization. Later studies showed [12] that the remaining electrons can react on an even shorter timescale ($\sim 30 \text{ as}$), suggesting that this response time might nevertheless depend on the degree of correlation.

Here we show that this response time can also be sensitive to the structural differences in the same molecule. For this purpose we studied the evolution of the charge density of the hole left by a sudden removal of different electrons from two tautomers of the uracil molecule (**U**) using a high-level *ab initio* methodology. Our results show that the early time evolution of the hole density can be different in the different tautomers and can depend on the symmetry of the ionized orbital. These findings suggest that even on such an ultra-short timescale of just a few tens of attoseconds, the charge dynamics can be characteristic for the system. We note that the subsequent femtosecond evolution of the electronic cloud of these cationic uracil tautomers is reported in Ref. [13].

II. THEORY AND COMPUTATIONAL DETAILS

As we want to study the response of the electronic cloud to a perturbation without explicitly taking into account the perturbation itself, it is convenient to consider a sudden ionization, as done in the original work of Breidbach and Cederbaum [10]. The assumption is that one can suddenly remove an electron from the system, which will create a nonstationary state at time $t = 0$ that will start to evolve under the cationic Hamiltonian. Theoretically, the initial state can be created by applying an electron annihilation operator \hat{a}_i on the electronic ground state $|\Psi_0\rangle$. It is also convenient to use

*mousumi.upadhyaykahaly@eli-alps.hu

†alexander.kuleff@pci.uni-heidelberg.de

the molecular Hartree-Fock orbitals as one-particle basis, in which case the operator \hat{a}_i simply removes an electron from the i th molecular orbital (MO). This is the so-called sudden approximation (see, e.g., Refs. [14,15]), which has been widely used in the last decades to analyze ionization spectra of atomic and molecular systems (see, e.g., Refs. [16–18]). As the dynamics we would like to study are solely due to the electron correlation, it is crucial that the method used to construct the cationic Hamiltonian describes the many-body effects as well as possible.

Especially suitable for this purpose are the methods based on the one-particle Green’s function or electron propagator, which have the advantage to provide a balanced treatment of the correlation effects in both the ground and ionic states, as well as a direct access to the full cationic spectrum in a single run, in contrast to other quantum chemistry methods for obtaining cationic states [19]. In this work we use the third-order non-Dyson algebraic diagrammatic construction [ADC(3)] scheme [20] for approximating the one-particle Green’s function [21]. The method has been shown to provide highly accurate photoionization spectra in various molecules [22–24].

In order to trace the response of the system upon ionization, we computed the time-dependent hole density $Q(\vec{r}, t)$ [6,25], defined as the difference between the electronic density of the system before ionization, $\rho_0(\vec{r})$, and that after removing an electron from the respective MO, $\rho_i(\vec{r}, t)$:

$$Q(\vec{r}, t) = \underbrace{\langle \Psi_0 | \hat{\rho} | \Psi_0 \rangle}_{\rho_0(\vec{r})} - \underbrace{\langle \Phi_i(t) | \hat{\rho} | \Phi_i(t) \rangle}_{\rho_i(\vec{r}, t)}. \quad (1)$$

In the above equation, $|\Psi_0\rangle$ is the electronic ground state of the system, and $|\Phi_i(t)\rangle$ is the nonstationary state created by suddenly removing an electron out of the i th MO. In the Heisenberg picture, the time-dependent electronic density can thus be written as

$$\rho_i(\vec{r}, t) = \langle \Phi_i(0) | e^{i\hat{H}t} \hat{\rho} e^{-i\hat{H}t} | \Phi_i(0) \rangle, \quad (2)$$

where \hat{H} is the cationic Hamiltonian of the system. Using the molecular orbitals of the neutral system as a basis, one can obtain the following expression for the hole density [25]:

$$Q(\vec{r}, t) = \sum_p |\tilde{\varphi}_p(\vec{r}, t)|^2 \tilde{n}_p(t), \quad (3)$$

where $\tilde{\varphi}_p(\vec{r}, t)$ are the natural charge orbitals and $\tilde{n}_p(t)$ their hole-occupation numbers. At each time point, the natural charge orbitals are different expansions in the neutral MO basis set. The present calculations were performed using the multielectronic wave-packet propagation technique [26]. The method uses the non-Dyson ADC(3) scheme to build the cationic Hamiltonian [20], employed then to propagate the initial state via the short iterative Lanczos technique [27,28]. Further technical and theoretical details about construction and analysis of the hole density can be found in Refs. [25,26,29].

The procedure sketched above has been applied to two of the lowest-energy tautomers of the uracil molecule. The molecular geometries were optimized at the PBE0/def2-TZVP level of theory, and the Hartree-Fock MOs, orbital energies, and two-electron integrals, needed for construct-

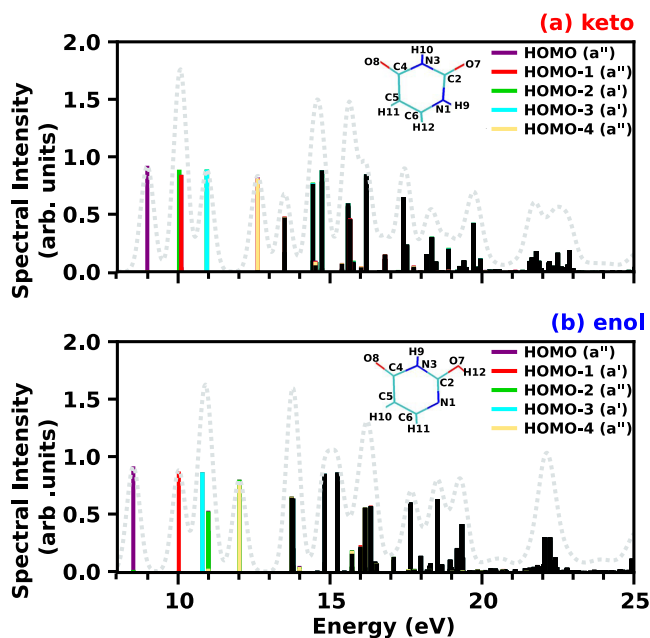


FIG. 1. Ionization spectra of keto-U (a) and enol-U (b) computed using the Green’s function non-Dyson ADC(3) approach. Each vertical line represents a cationic eigenstate with position corresponding to its ionization energy and spectral intensity proportional to its ionization cross section. The states populated by the removal of an electron from one of the highest five molecular orbitals and investigated in this work are color-coded. To account for the vibrational broadening, the spectra have been convoluted with a Gaussian with FWHM of 0.4 eV. The result is shown with a dashed grey line.

ing the ADC cationic Hamiltonian, were generated with the GAMESS-UK package [30] using cc-pVDZ basis set [31].

III. RESULTS AND DISCUSSION

Uracil (U) is one of the four chemical nitrogenous bases of RNA and has multiple tautomeric forms [32], among which the most stable ones (energy difference of 0.48 eV) are “keto-U” and “enol-U.” In keto-U (with two carboxyl groups) the tautomeric hydrogen (H9) bonds with nitrogen (N1), while in enol-U (with one carboxyl group and one hydroxyl group) the tautomeric hydrogen (H12) bonds with oxygen (O7); see the structures in Figs. 1(a) and 1(b), respectively. The hydrogen, denoted as H9 in keto-U and H12 in enol-U (see Fig. 1), is referred to as tautomeric hydrogen (Ht) throughout this paper. Both these tautomers are found in C_s symmetry and thus have two types of orbitals, symmetric (a') and antisymmetric (a''), with respect to the molecular plane.

The ionization spectra of keto-U and enol-U, computed at ADC(3)/cc-pVDZ level, are shown in Figs. 1(a) and 1(b), respectively. Each vertical line in these spectra represents a cationic eigenstate with position corresponding to its ionization energy and height, or spectral intensity, proportional to its ionization cross section. In a configuration-interaction picture, each normalized cationic state is represented as a sum of all contributing one-hole (1h) configurations, two-hole-one-particle (2h1p) configurations, etc., with the spectral intensity given by the sum of the weights of all contributing 1h

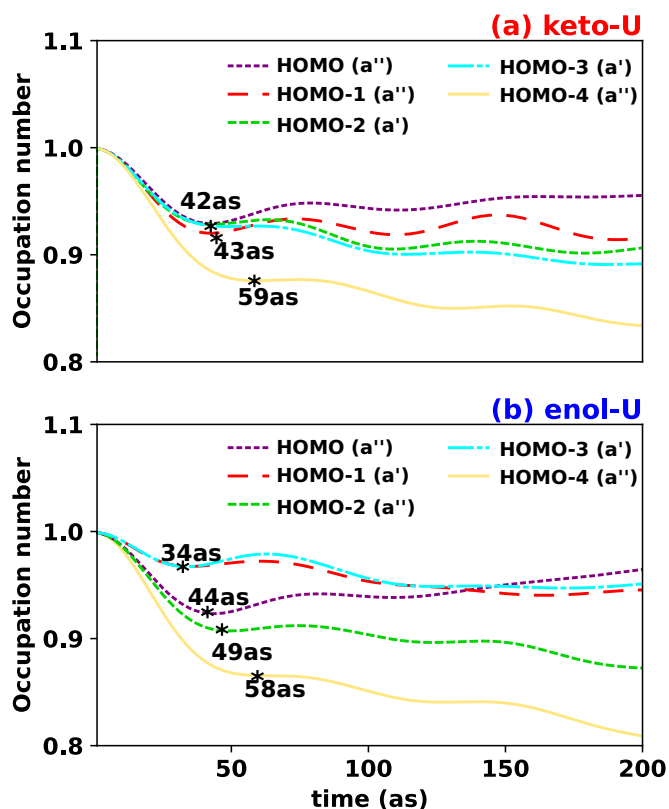


FIG. 2. Temporal evolution during the first 200 as of the hole-occupation numbers $\tilde{n}_i(t)$, Eq. (3), after ionization out of the five highest occupied molecular orbitals. The corresponding response times, defined as the first stationary point in the corresponding $\tilde{n}_i(t)$ curve, are marked with “*”.

configurations [3]. As the 2h1p and the higher configurations describe excitations on top of the removal of a particular electron, their weight is a measure of the correlation effects contributing to the corresponding state. Although not important for the present study, in order to mimic an experimental photoelectron spectrum and thus facilitate comparison with measured data, each line has been convoluted with a Gaussian having a FWHM of 0.4 eV to account for the vibrational broadening and experimental resolution. The result is depicted in Fig. 1 with a gray dashed curve.

The first few lines (up to about 15 eV) have large spectral intensities and thus correspond to states in which the correlation effects are relatively small. This is also the regime for which the third-order non-Dyson ADC approach used [ADC(3)] is the most accurate [23]. We will, therefore, perform electron-dynamics calculations in order to simulate the response of the electronic cloud to the removal of an electron from the highest five molecular orbitals (MOs), leading mainly to the population of the cationic states in this region (see Fig. 1, where these states are depicted in color).

Let us now examine the response of the two uracil tautomers upon ionization out of the five highest occupied MOs. Figure 2 shows the first 200 as of the evolution of the hole-occupation numbers $\tilde{n}_i(t)$ of the natural charge orbitals bearing the initial hole in each of the studied cases, see Eq. (3). We see that for every initial hole the short-time

behavior of $\tilde{n}_i(t)$ is very similar, namely, the hole occupation smoothly decreases until it reaches a stationary point, after which the evolution might continue differently. In order to compare the timescale of the response, we can, therefore, define the response time as time for which $\tilde{n}_i(t)$ reaches its first stationary point. Examining the two a' orbitals in both keto-U (HOMO – 2, HOMO – 3) and enol-U (HOMO – 1, HOMO – 3), we see that although their overall behavior is very similar, the response time is substantially shorter in enol-U (34 as) compared to that in keto-U (42 as). The difference between the tautomers is much less pronounced if we compare the a'' orbitals: HOMO, HOMO – 1, and HOMO – 4 in keto-U, and HOMO, HOMO – 2, and HOMO – 4 in enol-U. However, the different a'' orbitals show different response times, varying from about 40 to about 60 as. Interestingly, the response time increases when going deeper in the electronic shells, but at the same time a larger fraction of the initial hole gets filled during these first instances. We will return to this point below.

Overall, the creation of an a' hole shows a faster response than when an a'' electron is removed. A possible explanation of this observation could be that the σ orbitals of the molecular skeleton belong to the a' irreducible representation, which facilitates the overlap between the MOs of this symmetry [33] and thus the interaction between the electrons belonging to these orbitals. We can therefore expect that in more conjugated systems, in which the atoms are connected by alternating π bonds, the time needed for the electronic cloud to respond to a sudden perturbation will be shorter than in less conjugated molecules. A dependence of the timescale of an electronic process on the degree of electron correlation has been recently observed in the study of nonlocal electronic decays through carbon chains [34]. It is nevertheless remarkable to see that hints for such a dependence exist already in the immediate response of the electronic cloud to the removal of an electron.

In order to investigate further the differences in the response of the two tautomers upon sudden ionization, it is insightful to analyze the evolution of the hole density and its variation around each atomic site. Snapshots of the evolution of the hole density during the first 60 as following ionization out of the orbitals belonging to a' symmetry are shown in Fig. 3. We see that the sudden removal of an electron from the highest a' MO leads to a very similar response in the two tautomers, Figs. 3(a) and 3(c). Electron density (depicted in red in Fig. 3) starts to build up mainly around O8 and C4, as well as around C5 and N3, while the hole density increases around the N3-C2 and C6-C5 bonds, as well as around all hydrogen atoms. The removal of an electron from the next a' MOs triggers different dynamics in the two molecules. The respective orbitals are localized on different sites of the molecules—in keto-U the hole is mostly around O7, while in enol-U it is around N1 [see Figs. 3(b) and 3(d)]. The response in keto-U represents a transfer of electron density from C6-H12 to O7-C2 with an excess of electron density forming around N1. In enol-U, the filling of the exchange-correlation hole is mainly coming from electrons around H9-N3 and O7-Ht. Electron density accumulates also around C2 and C6.

The response of the electronic cloud to the sudden removal of the three outermost a'' orbitals shows similar tendencies.

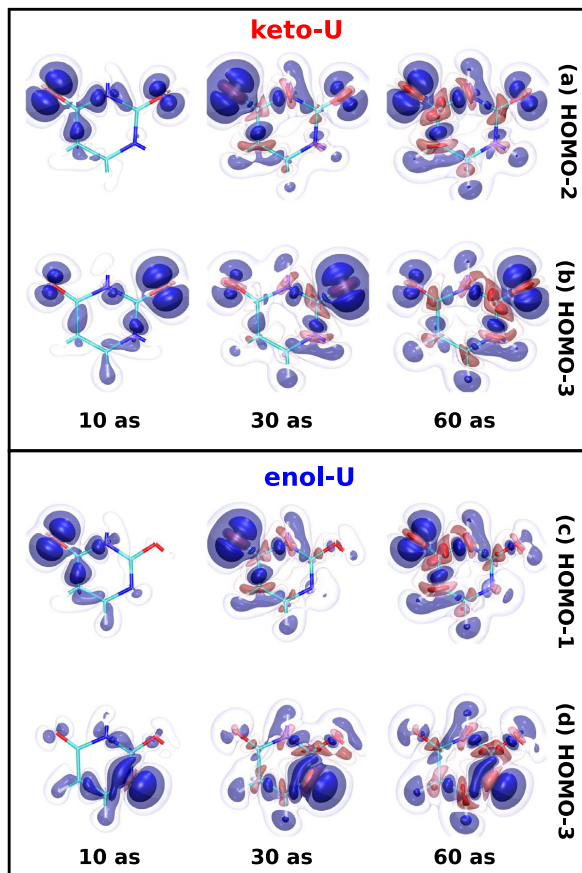


FIG. 3. Snapshots of the evolution of the hole density, following sudden ionization out of the two outermost molecular orbitals belonging to a' symmetry, (a, b) in keto-U and (c, d) in enol-U at 10 as, 30 as, and 60 as. The hole density is depicted in blue and the electron density, or the regions with excess of electrons, in red (isosurface values for surface with decreasing opacity: ± 0.0128 arb. units, ± 0.0032 arb. units, and ± 0.0008 arb. units).

The snapshots of the respective hole density evolution can be found in the Supplemental Material (SM), Fig. S1 [35]. Electronic density builds up around the atom where the largest fraction of the initial hole has been localized and around the atoms in its immediate proximity. The electron flow is mostly from regions not showing significant hole density initially, confirming that the dynamics mostly represent the filling of the exchange-correlation hole of the initial vacancy. Again, the density variations in keto-U are somewhat stronger than in enol-U, and the tautomeric hydrogen is usually an electron donor (except for HOMO) in the process. Note that the difference in the response times could be related to the symmetry of the orbitals or to a combination of the symmetry and position of tautomeric hydrogen. Further studies are needed to be able to fully clarify this issue.

In order to better compare the density variations around the different atoms, we computed the rate of these variations. As soon as the electron dynamics is initiated by the sudden ionization, the hole charge around the atoms in the molecule will start either to increase or decrease. If the positive charge decreases, then the flow of electrons is towards the corresponding atom, while if it increases the flow is away from

TABLE I. The overall electronic response time to the removal of an electron from the five outermost molecular orbitals of keto-U and enol-U, and the maximum variation time (τ) at the atomic site with the highest charge density response given in brackets.

Tautomer	Molecular orbital	Symmetry	response time [as]	Maximum variation time [as] (atom)
keto-U	HOMO	a''	42	24 (N1)
	HOMO - 1	a''	43	18 (O7)
	HOMO - 2	a'	42	18 (O8)
	HOMO - 3	a'	42	18 (O7)
	HOMO - 4	a''	59	18 (O7)
enol-U	HOMO	a''	44	24 (N1)
	HOMO - 1	a'	34	18 (O8)
	HOMO - 2	a''	49	19 (O7)
	HOMO - 3	a'	34	21 (N1)
	HOMO - 4	a''	58	17 (O7)

the atom. To capture this reaction to the sudden ionization, we computed the time needed to reach the maximum rate of density change. This can be termed a maximum-variation time, τ , and can be defined as the first minimum or maximum in $\frac{\partial Q(\vec{r},t)}{\partial t}$. The time evolution of the quantities $\frac{\partial Q(\vec{r},t)}{\partial t}$ are depicted in Figs. S2 in the SM [35]. The maximum variation time can be an important measure of the local correlation effects, as it shows the timescale on which a given atomic site starts to donate or receive electronic density.

It is intuitively clear that this property is related to the electronegativity of the corresponding atom. Indeed, the maximum variation time at the oxygen is always somewhat shorter than that at the nitrogen, and the largest density variations are observed at the sites characterized by higher electronegativity, like N and O (see Table I, where the maximum variation times at the sites of largest density change are listed). Moreover, the electron density flow is preferentially from the sites with lower electronegativity (carbon and hydrogen) to the sites with a higher one (oxygen and nitrogen). The closer comparison of the rates of change at the respective sites between the two tautomers reveals, however, some differences. Apart from the ionization out of the HOMO, the electronic cloud around the tautomeric hydrogen always responds differently in the two tautomers. The rate of density variation shows that Ht is an electron donor. The maximum variation time at Ht is typically reached faster in enol-U than in keto-U. It is striking to see that even with such a simple analytic approach local differences in the response of a molecule to a sudden ionization can be observed. We hope that these results will motivate further studies based on more refined analytic tools like, for example, Bader/QAIM analysis [36] or Mulliken charges [37].

Let us now return to the observed increase in the response time when the hole is created in deeper a'' orbitals (see Fig. 2). Going deeper into the electronic shells typically increases the correlation effects and thus one would expect the opposite trend, i.e., a decrease of the response time. That the correlation effects increase in the present case can be deduced by the decreasing spectral intensity of the main lines populated by removing an electron from the corresponding a'' orbitals (see Fig. 1). As we mentioned above, the smaller the

spectral intensity of a given state, the larger the contribution of the $2h1p$ configurations describing the electron correlation. The analysis of the rate of variations at the individual sites shows, however, that although the overall partial filling of the initial vacancy proceeds slower, the maximum variation time is reached faster for the deeper-lying orbitals. For both tautomers we obtain that the maximum variation time changes from 24 as for HOMO to 17 as for HOMO – 4 (see Table I). This means that the process of filling of the exchange-correlation hole of the initial vacancy, especially when this vacancy is delocalized over several atomic sites, can be rather sensitive to the local correlation effects at the particular chemical element.

The calculations discussed above have been performed at a fixed nuclear geometry, and although it might be evident that the nuclear motion is too slow to influence the attosecond response of the electronic cloud, it is interesting how much the effect is sensitive to the momentary position of the nuclei at the time of ionization. To investigate this effect, we performed calculations at different nuclear geometries around the equilibrium one. Our calculations performed even at maximal deformations in the ground vibrational state along the different vibrational modes show no sensitivity of the response time to these small variations of the atomic positions. The zero-point energy spread of the molecular wave function therefore is not expected to smear out the effect.

IV. SUMMARY AND CONCLUSION

Our results show that the response of the electronic cloud of a molecular system to a sudden perturbation is not universal and might depend on the strength of the electron correlation, the symmetry for the involved molecular orbitals, and the molecular structure. Although the two studied tautomers of **U** are structurally and electronically similar, the time that the remaining electrons need to respond to a sudden removal of the two outermost σ electrons can be quite different (~ 42 as in keto-**U** versus ~ 34 as in enol-**U**). Moreover, a careful analysis of the local variations of the electronic cloud clearly suggests that the process of filling of the exchange-correlation hole can be sensitive to the degree of correlation at the given site and that the flow of electronic density is typically from atoms with lower electronegativity to atoms with a higher one. A prominent example of the latter is the response of the

tautomeric hydrogen, which is a donor of electronic density (except in the case of HOMO), but the time and the degree of density variations are different in the different cases studied. All this clearly demonstrates that computing and analyzing the response of a molecule to a sudden removal of an outer-valence electron can be a valuable source of information on the overall strength of the correlation effects in the studied system and their distribution among the system constituents.

Before concluding, we would like to touch upon the possibility for an experimental investigation of the ultrafast response of the electronic cloud to a sudden perturbation. To be able to study such effects experimentally, we should be able to both “suddenly” remove an electron from the system and then measure the following ultrafast charge redistribution with an extreme precision. Although each of these prerequisites can be achieved to some extent, to the best of our knowledge, currently there are no developed techniques that can satisfy both conditions. The sudden-ionization limit can be approached, for example, by ionization with a high-energy photon [38], in which case the ionized electron leaves the interaction region nearly instantaneously due to its high kinetic energy. In the present context, ionization with soft x-rays would be needed. Different interferometric techniques have been used to measure photoionization time delays [39–41] that have provided unprecedented precision within several attoseconds. Even zeptosecond accuracy was recently achieved in measuring single-photon two-electron ionization of H_2 [42]. Nevertheless, a direct measurement of the response of the electronic cloud to a sudden ionization will be very challenging and thus will represent a stringent test for the fast developing attosecond technology.

ACKNOWLEDGMENTS

ELI-ALPS is supported by the European Union and cofinanced by the European Regional Development Fund (GINOP-2.3.6-15-2015-00001). K.C. and M.U.K. acknowledge the PaNOSC European project and Project No. 2019-2.1.13-TÉT-IN-2020-00059, which has been implemented with the support provided from the National Research, Development and Innovation Fund of Hungary, financed under the 2019-2.1.13-TÉT-IN funding scheme. V.D. and A.I.K. acknowledge financial support from the DFG through the QUTIF priority Program (SPP 1840).

-
- [1] G. Sansone, T. Pfeifer, K. Simeonidis, and A. I. Kuleff, Electron correlation in real time, *ChemPhysChem* **13**, 661 (2012).
 - [2] A. Temkin and A. Bhatia, Autoionization, in *Springer Handbook of Atomic, Molecular, and Optical Physics*, edited by G. Drake (Springer, New York, 2006), Chap. 25, pp. 391–399.
 - [3] L. Cederbaum, W. Domcke, J. Schirmer, and W. Von Niessen, Correlation effects in the ionization of molecules: Breakdown of the molecular orbital picture, *Adv. Chem. Phys.* **65**, 115 (1986).
 - [4] G. D. Scholes, Long-range resonance energy transfer in molecular systems, *Annu. Rev. Phys. Chem.* **54**, 57 (2003).
 - [5] T. Jahnke, U. Hergenbahn, B. Winter, R. Dörner, U. Fröhling, P. V. Demekhin, K. Gokhberg, L. S. Cederbaum, A. Ehresmann, A. Knie, and A. Dreuw, Interatomic and intermolecular Coulombic decay, *Chem. Rev.* **120**, 11295 (2020).
 - [6] L. S. Cederbaum and J. Zobeley, Ultrafast charge migration by electron correlation, *Chem. Phys. Lett.* **307**, 205 (1999).
 - [7] A. I. Kuleff, Ultrafast electron dynamics as a route to explore chemical processes, in *Attosecond Molecular Dynamics* (The Royal Society of Chemistry, London, 2018), Chap. 4, pp. 103–138.
 - [8] F. Calegari, G. Sansone, S. Stagira, C. Vozzi, and M. Nisoli, Advances in attosecond science, *J. Phys. B: At. Mol. Opt. Phys.* **49**, 062001 (2016).
 - [9] K. Ramasesha, S. R. Leone, and D. M. Neumark, Real-time probing of electron dynamics using attosecond time-resolved spectroscopy, *Annu. Rev. Phys. Chem.* **67**, 41 (2016).

- [10] J. Breidbach and L. S. Cederbaum, Universal Attosecond Response to the Removal of an Electron, *Phys. Rev. Lett.* **94**, 033901 (2005).
- [11] R. G. Parr and W. Yang, *Density Functional Theory of Atoms and Molecules* (Oxford University Press, Oxford, England, 1989).
- [12] A. I. Kuleff and L. S. Cederbaum, Tracing Ultrafast Interatomic Electronic Decay Processes in Real Time and Space, *Phys. Rev. Lett.* **98**, 083201 (2007).
- [13] K. Chordiya, V. Despré, B. Nagyillés, F. Zeller, Z. Diveki, A. I. Kuleff, and M. U. Kahaly, Photo-ionization initiated differential ultrafast charge migration: Impact of molecular symmetries and tautomeric forms, [arXiv:2203.02698](https://arxiv.org/abs/2203.02698).
- [14] R. Manne and T. Åberg, Koopmans' theorem for inner-shell ionization, *Chem. Phys. Lett.* **7**, 282 (1970).
- [15] H. W. Meldner and J. D. Perez, Observability of rearrangement energies and relaxation times, *Phys. Rev. A* **4**, 1388 (1971).
- [16] M. S. Deleuze, A. B. Trofimov, and L. S. Cederbaum, Valence one-electron and shake-up ionization bands of polycyclic aromatic hydrocarbons. I. Benzene, naphthalene, anthracene, naphthacene, and pentacene, *J. Chem. Phys.* **115**, 5859 (2001).
- [17] S. Gozem, A. O. Gunina, T. Ichino, D. L. Osborn, J. F. Stanton, and A. I. Krylov, Photoelectron wave function in photoionization: Plane wave or Coulomb wave? *J. Phys. Chem. Lett.* **6**, 4532 (2015).
- [18] T. Moitra, S. Coriani, and P. Decleva, Capturing correlation effects on photoionization dynamics, *J. Chem. Theory Comput.* **17**, 5064 (2021).
- [19] J. Schirmer, *Many-Body Methods for Atoms, Molecules and Clusters* (Springer Nature, London, UK, 2018).
- [20] J. Schirmer, A. B. Trofimov, and G. Stelter, A non-Dyson third-order approximation scheme for the electron propagator, *J. Chem. Phys.* **109**, 4734 (1998).
- [21] J. Schirmer, L. S. Cederbaum, and O. Walter, New approach to the one-particle Green's function for finite Fermi systems, *Phys. Rev. A* **28**, 1237 (1983).
- [22] A. W. Potts, D. M. P. Holland, A. B. Trofimov, J. Schirmer, L. Karlsson, and K. Siegbahn, An experimental and theoretical study of the valence shell photoelectron spectra of purine and pyrimidine molecules, *J. Phys. B: At. Mol. Opt. Phys.* **36**, 3129 (2003).
- [23] A. B. Trofimov, J. Schirmer, V. B. Kobychiev, A. W. Potts, D. M. P. Holland, and L. Karlsson, Photoelectron spectra of the nucleobases cytosine, thymine and adenine, *J. Phys. B: At. Mol. Opt. Phys.* **39**, 305 (2006).
- [24] I. L. Zaytseva, A. B. Trofimov, J. Schirmer, O. Plekan, V. Feyrer, R. Richter, M. Coreno, and K. C. Prince, Theoretical and experimental study of valence-shell ionization spectra of guanine, *J. Phys. Chem. A* **113**, 15142 (2009).
- [25] J. Breidbach and L. S. Cederbaum, Migration of holes: Formalism, mechanisms, and illustrative applications, *J. Chem. Phys.* **118**, 3983 (2003).
- [26] A. I. Kuleff, J. Breidbach, and L. S. Cederbaum, Multielectron wave-packet propagation: General theory and application, *J. Chem. Phys.* **123**, 044111 (2005).
- [27] C. Leforestier, R. Bisseling, C. Cerjan, M. Feit, R. Friesner, A. Gulberg, A. Hammerich, G. Jolicard, W. Karrlein, H.-D. Meyer *et al.*, A comparison of different propagation schemes for the time dependent Schrödinger equation, *J. Comput. Phys.* **94**, 59 (1991).
- [28] T. J. Park and J. C. Light, Unitary quantum time evolution by iterative Lanczos reduction, *J. Chem. Phys.* **85**, 5870 (1986).
- [29] J. Breidbach and L. Cederbaum, Migration of holes: Numerical algorithms and implementation, *J. Chem. Phys.* **126**, 034101 (2007).
- [30] M. F. Guest, I. J. Bush, H. J. Van Dam, P. Sherwood, J. M. Thomas, J. H. Van Lenthe, R. W. Havenith, and J. Kendrick, The GAMESS-UK electronic structure package: Algorithms, developments and applications, *Mol. Phys.* **103**, 719 (2005).
- [31] T. H. Dunning Jr., Gaussian basis sets for use in correlated molecular calculations. I. The atoms boron through neon and hydrogen, *J. Chem. Phys.* **90**, 1007 (1989).
- [32] J. Rejnek, M. Hanus, M. Kabeláč, F. Ryjáček, and P. Hobza, Correlated ab initio study of nucleic acid bases and their tautomers in the gas phase, in a microhydrated environment and in aqueous solution. Part 4. Uracil and thymine, *Phys. Chem. Chem. Phys.* **7**, 2006 (2005).
- [33] R. Hoffmann, Interaction of orbitals through space and through bonds, *Acc. Chem. Res.* **4**, 1 (1971).
- [34] J. B. Mullenix, V. Despré, and A. I. Kuleff, Electronic decay through non-linear carbon chains, *J. Phys. B: At. Mol. Opt. Phys.* **53**, 184006 (2020).
- [35] See Supplemental Material at <http://link.aps.org/supplemental/10.1103/PhysRevA.105.062808> for evolution of the hole density after ionization out of a" orbitals, and rate of change in the hole density at selected molecular sites.
- [36] R. F. W. Bader, *Atoms in Molecules: A Quantum Theory* (Clarendon Press, Oxford, 1990).
- [37] R. S. Mulliken, Electronic population analysis on LCAO-MO molecular wave functions. II. Overlap populations, bond orders, and covalent bond energies, *J. Chem. Phys.* **23**, 1841 (1955).
- [38] L. S. Cederbaum and W. Domcke, Theoretical aspects of ionization potentials and photoelectron spectroscopy: A Green's function approach, *Adv. Chem. Phys.* **36**, 205 (1977).
- [39] M. Schultze, M. Fieß, N. Karpowicz, J. Gagnon, M. Korbman, M. Hofstetter, S. Neppl, A. L. Cavalieri, Y. Komninos, T. Mercouris, C. A. Nicolaides, R. Pazourek, S. Nagele, J. Feist, J. Burgdörfer, A. M. Azzeer, R. Ernstorfer, R. Kienberger, U. Kleineberg, E. Goulielmakis *et al.*, Delay in photoemission, *Science* **328**, 1658 (2010).
- [40] K. Klünder, J. M. Dahlström, M. Gisselbrecht, T. Fordell, M. Swoboda, D. Guénot, P. Johnsson, J. Caillat, J. Mauritsson, A. Maquet, R. Taïeb, and A. L'Huillier, Probing Single-Photon Ionization on the Attosecond Time Scale, *Phys. Rev. Lett.* **106**, 143002 (2011).
- [41] P. Eckle, A. N. Pfeiffer, C. Cirelli, A. Staudte, R. Dörner, H. G. Muller, M. Büttiker, and U. Keller, Attosecond ionization and tunneling delay time measurements in helium, *Science* **322**, 1525 (2008).
- [42] S. Grundmann, D. Trabert, K. Fehre, N. Strenger, A. Pier, L. Kaiser, M. Kircher, M. Weller, S. Eckart, L. P. H. Schmidt, F. Trinter, T. Jahnke, M. S. Schöffler, and R. Dörner, Zeptosecond birth time delay in molecular photoionization, *Science* **370**, 339 (2020).